Published in final edited form as:
Ultrasound Med Biol. 2011 July ; 37(7): 1161–1169. doi:10.1016/j.ultrasmedbio.2011.04.012.

High-frequency ultrasound imaging for longitudinal evaluation of non-alcoholic fatty liver disease progression in mice

Itziar Fernández-Domínguez[1], **J Javier Echevarria-Uraga**[2], **Nieves Gómez**[3], **Zigmund Luka**[4], **Conrad Wagner**[4], **Shelly C Lu**[5], **José M Mato**[6], **Maria L Martínez-Chantar**[†,6], and **Juan Rodríguez-Cuesta**[†,1]

[1]Animal Unit, Biosciences Cooperative Research Centre (CIC bioGUNE), 48160-Bizkaia, Spain.

[2]Radiology Department, Galdakao-Usánsolo Hospital, 48960-Bizkaia, Spain.

[3]Animal Pathology Department, Neiker-Tecnalia, 48160-Bizkaia, Spain.

[4]Department of Biochemistry, Vanderbilt University, Nashville, TN 37232-0146, USA.

[5]Department of Biochemistry and Molecular Biology, Keck School of Medicine, University of Southern California, Los Angeles, CA 90089-9176, USA.

[6]Metabolomics Unit, Biosciences Cooperative Research Centre (CIC bioGUNE), 48160-Bizkaia, Spain.

Abstract

Non-alcoholic fatty liver disease (NAFLD) is one of the most common causes of hepatic damage in developed countries. For this reason, mouse models of NAFLD have been developed in which the progression of the disease assembling perfectly the human pathology. Here we show that diagnostic high-frequency ultrasound imaging (US) may be used as an effective method for monitoring the progression of liver disease, from steatosis to hepatocellular carcinoma in the methionine adenosyl transferase (MAT1A) and glycine N-methyltransferase (GNMT) deficient mice models. US reliably detected murine liver lesions associated to NAFLD in the two mice strains tested, with excellent agreement among US images, gross pathology, and histological sections. Our results suggest US as a relevant approach for the study of NAFLD in mice, with interesting technical and therapeutic implications.

Keywords

Ultrasonography; Hepatic pathology; NASH; Animal models; HCC

Contact information, María L Martínez-Chantar, Technologic Park of Biscay, Bulding 801-A, Biosciences Cooperative Research Centre, (CIC bioGUNE), 48160 Derio-Bizkaia, Spain. Telephone: ++34 944061318, Fax: ++34 944061301, mlmartinez@cicbiogune.es.
[†]MLM-C and JR-C share the senior authorship.

Introduction

Non-alcoholic fatty liver disease (NAFLD) is a condition where fat deposits in the liver and refers to a wide spectrum of disorders ranging from fatty liver (steatosis), to inflammation-derived non-alcoholic steatohepatitis (NASH) and which can progress into cirrhosis and hepatocellular carcinoma (HCC) (Diehl 1999; Lewis and Mohanty 2010). Insulin resistance, oxidative stress and inflammatory cascades are believed to play integral roles in the pathogenesis and progression of the disease, but the whole factors implicated in the progression of the disease are poorly understood (Jiang and Torok 2008, Lewis and Mohanty 2010). NAFLD, is one of the most common causes of hepatic damage in developed countries where is considered to be an emergent disease, with a prevalence in general population ranging from 10% to 20% (Lewis and Mohanty 2010). Regarding HCC, it is the fifth most common cancer in the world, accounting for an estimated 500,000 deaths annually (Parkin et al. 2001). This high mortality rates are mainly because often precancerous lesions are asymptomatic and therefore most HCCs are diagnosed at an advanced stage being that most patients die within 1 year of diagnosis (Doval et al. 2008). Currently, liver biopsy is the only safe test to assess an accurate diagnosis of the NAFLD stage and severity. Therefore, non-invasive techniques capable of predicting an early identification of the disease and assess the HCC risk with no necessity for biopsy are needed. The literature contains numerous rodent models to study steatosis, NASH and HCC (Varela-Rey et al. 2009). Those models are extremely useful and so far have given us invaluable information of the mechanisms involved in NAFLD development (Diehl 2005; Koteish and Diehl 2001). The challenge now is to identify common mechanisms in humans to improve prognosis and treatment of the disease.

In this context, there have been previously described abnormalities in the methionine metabolism in several models of NAFLD and also in patients with liver disease. Both high and low levels of SAMe predispose to liver injury (Martinez-Lopez et al. 2008). In this regard, mouse models of liver disease have been developed in which the proteins responsible for SAMe synthesis, methionine adenosyl transferase (MAT1A gene) and catabolism, glycine N-methyltransferase (GNMT gene) respectively, have been inactivated (Lu et al. 2001; Martinez-Chantar et al. 2008). Those KO mice develop steatosis, NASH, cirrhosis and HCC and both closely replicate the progression of NAFLD in humans, which makes them extremely useful to elucidate the mechanism underlying liver disease and new approaches for prognosis and diagnosis of this pathology.

Ultrasound imaging (US) is a versatile, well-established, and widely used diagnostic tool in human and veterinary medicine (Coatney 2001). Importantly, the benefit of employing US in the diagnosis and monitoring of NAFLD in mice has never been defined. In this study, we describe the usefulness of ultrasounds for assessing liver lesions associated to NAFLD in MAT1A and GNMT KO mice.

Materials and Methods

Animals

All the procedures with animals were carried out at the SPF animal facility of CIC bioGUNE (AAALAC-accredited) and conducted in accordance with *The Guide for the Care and Use of Laboratory Animals* (Institute of Laboratory Animal Resources 1996) and with European policies (European Commission 1986). Ten GNMT-KO and ten MAT1A-KO male 8 weeks old mice and their respective controls (20 wild type mice), were obtained from the animal facility of CIC bioGUNE. Animals were housed in groups of five in polycarbonate cages containing wood chip bedding (Lignocel, HBK 1500–3000, JRS J. Rettenmaier & Söhne, Rosenberg, Germany) in a temperature (20–24°C) and relative

humidity (50–65%) controlled room with a 12:12 hour dark:light cycle (lights on 08:00h–20:00h), were fed with rodent maintenance diet (Ref. 2014, Harlan Teklad, UK) and provided with water *ad libitum*. The experimental protocol was approved by the Bioethical and Animal Welfare Committee of CIC bioGUNE.

Experimental design

US images were acquired in all mice monthly, from the age of 2 to 18 months. After sacrifice, additional US scans were performed on excised livers before final validation by histopathological analysis. Age matched control mice were sacrificed to confirm negative results at selected time points. Using this design, US data were validated and progression of the disease was monitored in all animals of the experimental cohort. At the end of the experiment, all remaining mice were sacrificed and examined to confirm US findings.

In vivo ultrasound imaging

For US, the Vevo 770 high-frequency ultrasound system (VisualSonics Inc., Toronto, Ontario, Canada) was used employing a 40-MHz probe (Scanhead RMV-704, VisualSonics Inc., Toronto, Ontario, Canada) with a 6-mm focal depth. During imaging sessions, mice were kept under anesthesia with 1.5% isoflurane in oxygen and restrained on a heated stage (THM-150, Indus Instruments, Houston, TX). Before each imaging session, mice's abdomen was depilated with commercial hair removal cream (Veet, Reckitt Benckifer, Granollers, Spain), an ultrasound coupling gel (Aquasonic 100, Parker Laboratories Inc., Fairfield, NJ) was applied to the depilated skin, and images of the liver were acquired through the ventral body wall in transverse and sagittal orientations. US images were acquired in a standardized manner and analyzed by two independent operators, who worked together to reach a consensus on image interpretationin in each experimental group (MAT1A-KO or GNMT-KO). After the imaging sessions, mice were allowed to recover completely in a cage over a thermal blanquet. All the animals were observed daily for signs of pain or discomfort.

Longitudinal evaluation of the liver by *in vivo* US

The liver parenchyma was examined for echogenicity, homogeneity, presence or absence of nodules, echostructure and border definition. When nodules were present, they were characterized in terms of echogenicity, echostructure, size and location. The size of the nodules was determined by caliper measurement of the longest diameter in the transverse view of the liver.

Confirmation of i*n vivo* US findings

To validate *in vivo* imaging findings, mice were sacrificed by cervical dislocation and their livers were excised immediately. For correlating the size and location of the lesions previously observed, visual inspection and *ex vivo* US of the liver were performed. After that, selected liver sections were fixed by immersion into a solution of 10% formaldehyde and paraffin-embedded. 4-μm-thick tissue sections were stained with hematoxylin-eosin (H/E), periodic acid-Schiff (PAS), Masson's trichrome and Sirius red stains. Finally, two independent veterinary pathologists performed the histopathological diagnosis of the lesions.

Results

High-frequency ultrasound-mediated imaging of normal liver architecture

Control mice showed homogeneous liver parenchyma, with medium level echogenicity and regular liver surface during the study. Left lobe, anterior and posterior portions of the right lobe, left and right portions of the medial lobe and caudate lobes of the liver could be

identified during US sessions. In addition, main abdominal vessels, such as the abdominal aorta, the caudal vena cava and the portal vein, could be distinguished.

Identification of murine liver lesions using high-frequency ultrasound

US reliably detected murine liver lesions associated to NAFLD in the experimental groups of the two mice strains tested, with excellent agreement among US images, gross pathology, and histological sections. Study results have been classified as non-neoplastic (Fig. 1) and neoplastic (Fig. 2) liver lesions. Their echographic features are described below.

Non-neoplastic liver lesions

Fatty Change—Steatosis in the liver showed different imaging patterns depending on the distribution of the fat deposition. By US the fatty hepatic parenchyma demonstrated increased echogenicity and attenuation; therefore, the echogenic walls of the portal and hepatic veins were difficult to distinguish. In this way, focal fatty change appeared in US as a single homogeneously hyperechoic focal lesion with well defined borders and no compression of the adjacent tissue (Fig. 1A). The multifocal form showed multiple and confluent homogeneously hyperechoic foci surrounded by areas of normal parenchyma (Fig. 1B). The diffuse presentation of the fatty change could be seen as a homogeneous hyperechoic area affecting entire lobes of the liver or well demarcated areas at specific localizations (Fig. 1C).

Biliary Cysts—US usually allowed us a confident diagnosis of a simple biliary cyst by showing a single homogeneously anechoic focal lesion with a thin wall and posterior acoustic enhancement (Fig. 1D). Other times, biliary cysts appeared in a multiloculated form showing multiple and confluent homogeneously anechoic foci in the hepatic parenchyma (Fig. 1E).

Cellular Alteration Foci—These foci are histologically defined as lesions comprised by hepatocytes which are cytomorphologically and tinctorially distinct from the surrounding parenchyma. Foci of cellular alteration vary in size, may be round or irregular in shape and cause no compression of the adjacent parenchyma. They appeared in US as patchy echotexture nodules with a non-well defined boundary and no mass effect (Fig. 1F). In our study, those patchy areas were correlated with fat containing hepatocytes (hyperechoic or bright areas) and cellular proliferation (hypo- or isoechoic areas).

Neoplastic liver lesions

Hepatocellular Adenoma—They are progressively growing well-circumscribed lesions which cause distinct compression of adjacent parenchyma and may bulge for the liver surface. The US image of this type of lesions usually showed a heterogeneous echotexture large nodule which compress adjacent tissue (Fig. 2A). Nevertheless, small adenomas showed homogeneous echotexture due to a more homogeneous pattern of fat deposition.

Hepatocellular Carcinoma—In this study it had been possible to observe hepatocellular carcinomas in different stages. US of early stage HCCs showed small hypoechoic nodules with a well defined boundary (Fig. 2B). Other times, HCC appeared in US as a mixed composition lesion containing hyper- and hypoechoic areas which correspond to fat deposition and neoplastic tissue. This composition formed a characteristic figure that is known as the mosaic pattern of HCC (Fig. 2C). Advanced stage HCCs were normally large and heterogeneous lesions with many different US appearances that depend on the amount of fat content, presence of necrosis or vascular structures (Fig. 2D and 2E).

Follow-up of individual liver lesions by non-invasive ultrasound imaging—US allowed us the detection and follow-up of hepatic lesions in single animals over the time. As an example, Figure 3 shows representative longitudinal series of US images of three nodules followed-up in the liver of one MAT1A-KO (Fig. 3A) and two GNMT-KO (Fig. 3B and 3C) mice. In all cases, borders of the nodules could be delimited based in the differences of echogenicity and echostructure between the lesions and the surrounding tissue. After their histopathologic examination, all those nodular lesions were diagnosed as HCCs surrounded by altered liver parenchyma.

Monitoring of NAFLD progression in MAT1A-KO and GNMT-KO mice—Ultrasonographic findings assessed and monitored over the time of the study, including the lesions associated to these findings and their incidence at selected time points are shown in Table 1.

A homogeneous and isoechoic hepatic parenchyma was observed in all mice of the control groups along the study (n=20) and in one animal from the experimental groups at the age of 3 months. In all cases, that US finding was macroscopically and histologically associated to normal hepatic parenchyma. Hepatic parenchyma of animals from the experimental groups became more and more heterogeneous with time. That heterogeneity of livers was associated to an unspecifically altered parenchymal architecture and in some cases, to fibrosis (Figure 4). Diffuse, focal or multifocal steatosis was always present in MAT1A-KO and GNMT-KO animals during the study, with higher incidence (around 50%) in the first 6 months. However, the distribution of the fatty change was widespread in the first months, becoming more localized and present in fewer animals while other lesions took its place. Anechoic nodules were associated to biliary cysts and were present in four GNMT-KO mice ranging from 12 to 18 months. Ultrasonographic findings which were associated to neoplastic lesions, started to appear at 6 months (mainly in GNMT-KO mice) and were present in 100% of the animals at 15 months.

Discussion

In the current work we studied the usefulness of US for *in vivo* detection of hepatic pathologies in two strains of mice, GNMT-KO and MAT1A-KO. These mice are well-characterized animal models of NAFLD (Lu et al. 2001, Martinez-Chantar et al. 2008) and spontaneously develop steatosis, NASH, cirrhosis and HCC, resembling the progression of the human disease. GNMT-KO mice develop steatosis at the age of 3 months, NASH at 5 months, may develop cirrhosis at 6 months and HCC at 8 months; while MAT1A-KO mice develop steatosis at 3 months, NASH at 8 months and HCC at 15 months. By using US, we have been able to detect different types of liver lesions associated to NAFLD and follow-up their progression in single animals over the time. Precisely, we have chosen time points 3, 5, 6, 8 and 15 months to show the progression of ultrasound findings and their associated lesions along the study (see Table 1).

US is a well proof non-invasive method for the detection of liver lesions in human (Maruyama and Ebara 2006) and veterinary medicine (Gaschen 2009). In the recent years it has been used to detect hepatic pathology in research animals (Echevarria-Uraga et al. 2010; Lessa et al. 2010; Lisi et al. 2003), including mice (Graham et al. 2005; Mai et al. 2004; Schmitz et al. 2004). Those studies were focused in the ultrasonographic study of specific pathologies such as metastases (Graham et al. 2005) or HCC (Mai et al. 2004, Schmitz et al. 2004), but to our knowledge this is the first report including a wide range of non-neoplastic and neoplastic hepatic lesions associated to NAFLD in mice.

Simple steatosis is the first lesion expected in the progression of NAFLD, therefore, fatty change was the first finding we could identify in our models from the age of 2 months. Furthermore, we describe different patterns of steatosis or fatty change in mice liver. As in humans, diffuse steatosis was easily diagnosed (see Fig. 1C) because the image interpretation was usually straightforward (Hamer et al. 2006). The diagnosis of focal and multifocal fat depositions was more difficult because imaging findings may resemble mass lesions (see Fig. 1A and 1B). Homogeneous hyperechogenicity within the nodule, absence of compression of the adjacent tissue and well defined regular borders were used as clues to diagnose focal steatosis in our study. Precisely, those findings have been proposed as signs for the diagnosis of this pattern of fat deposition in humans (Hamer et al. 2006).

In some cases, we observed lesions with similar characteristics of those of the focal fatty change, but with a composition that seemed to be more complex than simply fat and which grew with time becoming more heterogeneous. Those lesions were diagnosed as cellular alteration foci (see Fig. 1F) and have been reported to be an intermediate stage in the progression to hepatocellular adenomas and finally to HCC in rodents (Frith 1988).

Occasionally, we have observed biliary cysts in the liver of aging GNMT-KO mice. To our knowledge this is the first report in which simple and multiloculated biliary cysts are identified in mice by US. Ultrasonography usually allows a confident diagnosis of this lesion in human radiology (Bartolotta et al. 2009) and similarly, in mice. Biliary cysts have been described as very rare congenital lesions or as occasional findings in aging mice (Maronpot 1999). In humans, it has been previously reported that bile acids levels are increased in the liver of patients with NASH (Aranha et al. 2008). This situation could be related with the presence of this lesion in GNMT-KO mice, but further studies must be carried out to address this hypothesis. In any case, this is a clear example of the non-expected findings and additional information that US could provide to the study of NAFLD in animal models.

In human medicine it has been proposed a model of stepwise carcinogenesis for HCC which usually is triggering after the development of cirrhosis (Hussain et al. 2002). MAT1A-KO mice do not develop fibrosis, but GNMT-KO mice have echographic characteristics similar of those commonly described as fibrotic signs in animals (Lessa et al. 2010) and humans (Nishiura et al. 2005), such as increased echogenicity, heterogeneous parenchymal architecture and irregular hepatic surface. Interestingly, in our mice models the heterogeneity of the hepatic parenchyma became more frequent with time and was associated to a microscopically altered liver architecture (Figure 4). In our study we have succeed detecting different types of neoplastic lesions that have been related to the progression of HCC. In this sense, we have observed hepatocellular adenomas as heterogeneous echotexture nodules which cause compression of the adjacent parenchyma (see Fig. 2A). Some authors have suggested that fat deposition in adenomas is usually uniform while fat deposition in HCCs is patchy (Prasad et al. 2005). In this work, small adenomas (<3 mm) showed homogeneous fat deposition, but large adenomas (>3mm) revealed a heterogeneous deposition very similar to that observed in advanced stage HCCs. It has been described for humans that large hepatocellular adenomas appear heterogeneous in echography, reflecting the complex histological nature and composition of the lesions (Bartolotta et al. 2009), an observation that completely match with our findings in mice. However, unlike adenomas, advanced HCCs usually show other figures like necrotic caverns or vascular proliferation areas together with fat deposition, which makes the structure and US appearance of these lesions miscellaneous (Yu et al. 2004). In this study we have followed-up by US the progression of HCC through time and subsequently, observe HCC in different evolution stages. In this respect, we observed early stage HCCs as hypoechoic, homogeneous, small and roundish lesions with well defined borders (see Fig.

2B). The same ultrasonographic aspect has been reported both, in humans (Yu et al. 2004) and mice (Mai et al. 2004) for small HCCs. Those authors have also proposed that the tumour becomes non-homogeneous and hyperechoic when it grows in size, acquiring a characteristic mosaic pattern that we have shown in our results (see Fig. 2C). As we have mentioned above, HCC becomes more heterogeneous concomitantly with the loss of cellularity, and the appearance of angiogenic and necrotic areas. Consequently, advanced stage HCCs appeared in our study as large heterogeneous hyperechoic nodules with a mixed composition due to fatty change, necrosis or sinusoidal dilatation (see Figs. 2D and 2E). In some cases, advanced stage HCCs appeared as homogeneous isoechoic masses. This type of lesions might be difficult to distinguish from the normal liver parenchyma but indirect evidences such as compression, alteration of the normal liver structure or localized bulging of the hepatic surface should raise the suspicion of a HCC (Yu et al. 2004).

Summing up, serial US examination has allowed us to monitor the progression of NAFLD in GNMT-KO and MAT1A-KO mice livers from a status where no detectable pathology was observed, through the appearance of the first lesions, to the final development of advanced stage HCCs. In this respect, high-frequency ultrasound imaging has proved to be a useful tool for studying the dynamic growth of liver lesions in our models. US images were analyzed by two operators working in consensus, therefore, results were considered reliable only when there was an agreement between sonographers and findings were confirmed by histopathology. The observations made by US for GNMT-KO and MAT1A-KO strains are likely to be considered as indicators of the powerful information that this technology could provide for the study of NAFLD and similar hepatic pathologies in mice. In some cases, it may be difficult to establish the definitive nature of a finding because gray-scale ultrasound is considered a not specific technique in the diagnosis of focal liver lesions. A better understanding of liver pathologies associated to NAFLD could be achieved through the use of contrast-enhanced ultrasound, which may provide more accurate information almost likewise computed tomography and magnetic resonance imaging (Jang et al. 2009), so further approaches in this sense will be performed to optimize and expand the characteristics of this technology in our disease models. Nevertheless, currently we are successfully using conventional US in GNMT-KO and MAT1A-KO mice models for the detection of the optimal moment for the sacrifice of animals to obtain a determined cell type or to establish the starting point for new experimental treatments.

Based on our findings, it is really evident that US contributes to the refinement of the experimental technique against more invasive procedures, and allows the reduction of the number of animals in research, making possible an individual characterization of a hepatic lesion in a single animal over the time. Therefore, this technique may be used as a non-invasive tool to characterize the progression of NAFLD in mice, becoming a relevant approach during experimental treatment.

Acknowledgments

Acknowledgments / Financial support

AT-1576 (to M.L.M.-C and J.M.M), SAF2005-00855, HEPADIP-EULSHM-CT-205 and ETORTEK-2008 (to M.L.M.-C and J.M.M); ETORTEK 2009 EH (to M.L.M.-C and J.M.M); Sanidad Gobierno Vasco 2009 (to M.L.M.-C); NIH grant support DK080010 (to C.W). We also thank Dr James Sutherland for his assistance with the revision of this manuscript.

References

Aranha MM, Cortez-Pinto H, Costa A, da Silva IB, Camilo ME, de Moura MC, Rodrigues CM. Bile acid levels are increased in the liver of patients with steatohepatitis. Eur J Gastroenterol Hepatol. 2008; 20:519–525. [PubMed: 18467911]

Bartolotta TV, Taibbi A, Midiri M, Lagalla R. Focal liver lesions: contrast-enhanced ultrasound. Abdom Imaging. 2009; 34:193–209. [PubMed: 18317833]

Coatney RW. Ultrasound imaging: principles and applications in rodent research. ILAR J. 2001; 42:233–247. [PubMed: 11406722]

Diehl AM. Nonalcoholic steatohepatitis. Semin Liver Dis. 1999; 19:221–229. [PubMed: 10422202]

Diehl AM. Lessons from animal models of NASH. Hepatol Res. 2005; 33:138–144. [PubMed: 16198624]

Doval DC, Pande SB, Sharma JB, Pavithran K, Jena A, Vaid AK. Prometheus' spirit: quality survival in advanced hepatocellular carcinoma after gemcitabine and cisplatin-based chemotherapy. Singapore Med J. 2008; 49:e293–e295. [PubMed: 18946603]

Echevarria Uraga JJ, Garcia-Alonso Montoya I, Diaz Sanz I, Herrero de la Parte B, Miguelez Vidales JL, Zabalza Estevez I, Fernandez-Ruanova B. Ultrasonographic characterization of an experimental model of liver metastases from colon carcinoma in rats. Radiologia. 2010; 52:37–44. [PubMed: 19945720]

EuropeanCommission. Directive 86/609/EEC on the approximation of laws, regulations and administrative provisions of the member states regarding the protection of animals used for experimental and other scientific purposes. Off J Eur Commun. 1986; L358:1–29.

Frith, CHWJ. Color atlas of neoplastic and non-neoplastic lesions in aging mice. Gurnee, IL: Davis DVM Foundation; 1988.

Gaschen L. Update on hepatobiliary imaging. Vet Clin North Am Small Anim Pract. 2009; 39:439–467. [PubMed: 19524788]

Graham KC, Wirtzfeld LA, MacKenzie LT, Postenka CO, Groom AC, MacDonald IC, Fenster A, Lacefield JC, Chambers AF. Three-dimensional high-frequency ultrasound imaging for longitudinal evaluation of liver metastases in preclinical models. Cancer Res. 2005; 65:5231–5237. [PubMed: 15958568]

Hamer OW, Aguirre DA, Casola G, Lavine JE, Woenckhaus M, Sirlin CB. Fatty liver: imaging patterns and pitfalls. Radiographics. 2006; 26:1637–1653. [PubMed: 17102041]

Hussain SM, Zondervan PE, JN IJ, Schalm SW, de Man RA, Krestin GP. Benign versus malignant hepatic nodules: MR imaging findings with pathologic correlation. Radiographics. 2002; 22:1023–1036. discussion 37–9. [PubMed: 12235331]

Institute of Laboratory Animal Resources NRC. Guide for the care and use of laboratory animals. Washington D.C.: National Academy Press; 1996.

Jang HJ, Yu H, Kim TK. Contrast-enhanced ultrasound in the detection and characterization of liver tumors. Cancer Imaging. 2009; 9:96–103. [PubMed: 19933022]

Jiang J, Torok N. Nonalcoholic steatohepatitis and the metabolic syndrome. Metab Syndr Relat Disord. 2008; 6:1–7. [PubMed: 18370830]

Koteish A, Diehl AM. Animal models of steatosis. Semin Liver Dis. 2001; 21:89–104. [PubMed: 11296700]

Lessa AS, Paredes BD, Dias JV, Carvalho AB, Quintanilha LF, Takiya CM, Tura BR, Rezende GF, Campos de Carvalho AC, Resende CM, Goldenberg RC. Ultrasound imaging in an experimental model of fatty liver disease and cirrhosis in rats. BMC Vet Res. 2010; 6:6. [PubMed: 20113491]

Lewis JR, Mohanty SR. Nonalcoholic fatty liver disease: a review and update. Dig Dis Sci. 2010; 55:560–578. [PubMed: 20101463]

Lisi D, Kondili LA, Ramieri MT, Giuseppetti R, Bruni R, Della Rocca C, De Santis A, Rapicetta M. Ultrasonography in the study of hepatocellular carcinoma in woodchucks chronically infected with WHV. Lab Anim. 2003; 37:233–240. [PubMed: 12869286]

Lu SC, Alvarez L, Huang ZZ, Chen L, An W, Corrales FJ, Avila MA, Kanel G, Mato JM. Methionine adenosyltransferase 1A knockout mice are predisposed to liver injury and exhibit increased

expression of genes involved in proliferation. Proc Natl Acad Sci U S A. 2001; 98:5560–5565. [PubMed: 11320206]

Mai W, Barraud L, Lefrancois L, Scoazec JY, Guerret S, Vray D, Merle P, Vitvitski-Trepo L, Trepo C, Janier MF. Ultrasound detection of spontaneous hepato-cellular carcinomas in X/myc bitransgenic mice. Liver Int. 2004; 24:651–657. [PubMed: 15566518]

Maronpot, R. Pathology of the mouse. Vienna, IL: Cache River Press; 1999.

Martinez-Chantar ML, Vazquez-Chantada M, Ariz U, Martinez N, Varela M, Luka Z, Capdevila A, Rodriguez J, Aransay AM, Matthiesen R, Yang H, Calvisi DF, Esteller M, Fraga M, Lu SC, Wagner C, Mato JM. Loss of the glycine N-methyltransferase gene leads to steatosis and hepatocellular carcinoma in mice. Hepatology. 2008; 47:1191–1199. [PubMed: 18318442]

Martinez-Lopez N, Varela-Rey M, Ariz U, Embade N, Vazquez-Chantada M, Fernandez-Ramos D, Gomez-Santos L, Lu SC, Mato JM, Martinez-Chantar ML. S-adenosylmethionine and proliferation: new pathways, new targets. Biochem Soc Trans. 2008; 36:848–852. [PubMed: 18793149]

Maruyama H, Ebara M. Recent applications of ultrasound: diagnosis and treatment of hepatocellular carcinoma. Int J Clin Oncol. 2006; 11:258–267. [PubMed: 16937299]

Nishiura T, Watanabe H, Ito M, Matsuoka Y, Yano K, Daikoku M, Yatsuhashi H, Dohmen K, Ishibashi H. Ultrasound evaluation of the fibrosis stage in chronic liver disease by the simultaneous use of low and high frequency probes. Br J Radiol. 2005; 78:189–197. [PubMed: 15730982]

Parkin DM, Bray FI, Devesa SS. Cancer burden in the year 2000. The global picture. Eur J Cancer. 2001; 37 Suppl 8:S4–S66. [PubMed: 11602373]

Prasad SR, Wang H, Rosas H, Menias CO, Narra VR, Middleton WD, Heiken JP. Fat-containing lesions of the liver: radiologic-pathologic correlation. Radiographics. 2005; 25:321–331. [PubMed: 15798052]

Schmitz V, Tirado-Ledo L, Tiemann K, Raskopf E, Heinicke T, Ziske C, Gonzalez-Carmona MA, Rabe C, Wernert N, Prieto J, Qian C, Sauerbruch T, Caselmann WH. Establishment of an orthotopic tumour model for hepatocellular carcinoma and non-invasive in vivo tumour imaging by high resolution ultrasound in mice. J Hepatol. 2004; 40:787–791. [PubMed: 15094226]

Varela-Rey M, Embade N, Ariz U, Lu SC, Mato JM, Martinez-Chantar ML. Non-alcoholic steatohepatitis and animal models: understanding the human disease. Int J Biochem Cell Biol. 2009; 41:969–976. [PubMed: 19027869]

Yu SC, Yeung DT, So NM. Imaging features of hepatocellular carcinoma. Clin Radiol. 2004; 59:145–156. [PubMed: 14746783]

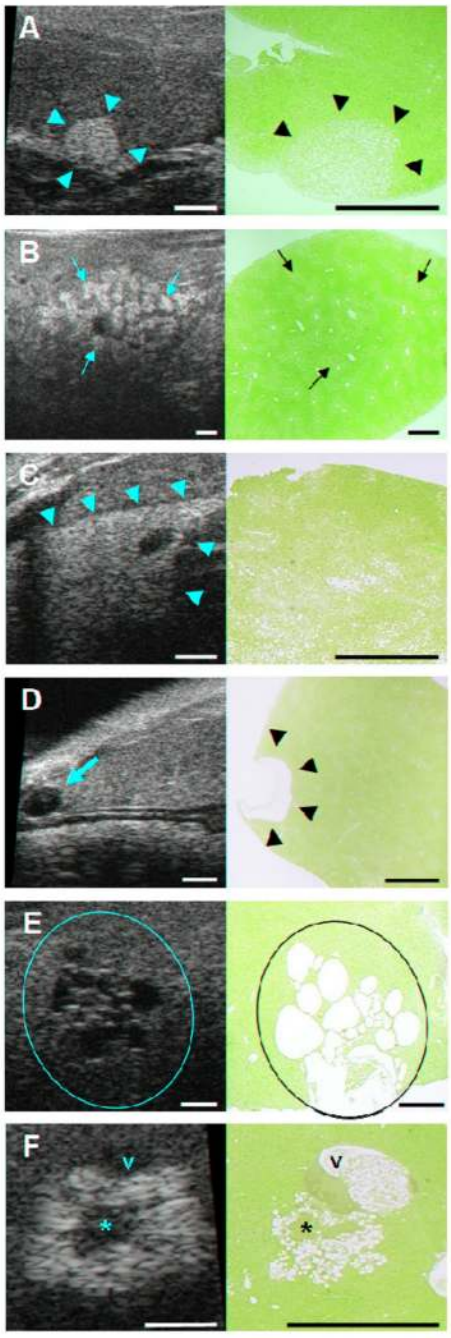

Figure 1. Identification of non-neoplastic liver lesions by high-frequency ultrasound imaging in GNMT-KO and MAT1A-KO mice

Ultrasound (US) images (left column) with corresponding H/E histologic sections (right column). The location of each lesion in US (yellow marks) and histologic sections (black marks) is indicated. Bars on US images and histologic sections, 1 mm. **A**, Focal fatty change in the caudate lobe of the liver of GNMT-KO (5 months). **B**, Multifocal fatty change in the right anterior lobe of the liver of MAT1A-KO (3 months). **C**, Diffuse fatty change in the left lobe of the liver of GNMT-KO (3 months). **D**, Simple biliary cyst in the left lobe of the liver of GNMT-KO (12 months). **E**, Multiloculated biliary cysts in the right posterior lobe of the

liver of GNMT-KO (13 months). **F**, Cellular alteration focus in the left lobe of the liver of MAT1A-KO (12 months). Portal vein (v) and cellular proliferation areas (*) are labeled.

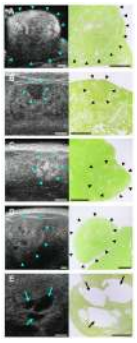

Figure 2. Identification of neoplastic liver lesions by high-frequency ultrasound imaging in GNMT-KO and MAT1-AKO mice

Ultrasound (US) images (left column) with corresponding H/E histologic sections (right column). The location of each lesion in the US (yellow arrows) and histologic sections (black arrows) is indicated. Bars on US images and histologic sections, 1 mm. **A**, Hepatocellular adenoma in the left lobe of the liver of MAT1A-KO (15 months). **B**, Early stage HCC in the left lobe of the liver of MAT1A-KO (15 months). **C**, Characteristic mosaic pattern of HCC in the left lobe of the liver of MAT1A-KO (15 months). **D**, Advanced stage HCC in the left lobe of the liver of MAT1A-KO (17 months). **E**, Vascular proliferation in an advanced stage HCC in the right medial lobe of the liver of GNMT-KO (9 months).

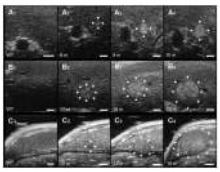

Figure 3. Follow-up of individual liver lesions by non-invasive ultrasound imaging

Representative ultrasound (US) images of the progression of HCC (A–C). First column of each image series (A1, B1, C1) shows a representative image of an adult control mouse liver. The location of the lesions in US (white arrows) is indicated. Bar on US images, 1 mm. **A**, Progression of an early stage HCC in MAT1A-KO. Maximum diameters of the HCC: A2, 0.45 mm (6 months); A3, 0.76 mm (9 months); A4, 1.07 mm (10 months). **B**, Progression of HCC from the mosaic pattern feature to a heterogeneous form in GNMT-KO. Maximum diameters of the HCC: B2, 1.21 mm (17 months); B3, 1.79 mm (19 months); B4, 2.96 mm (20 months). **C**, Progression of HCC from a homogeneous hypoechoic early stage to a large hyperechoic bulging form in GNMT-KO. Maximum diameters of the HCC: C2, 0.65 mm (15 months); C3, 2.27 mm (18 months); C4, 4.45 mm (19 months).

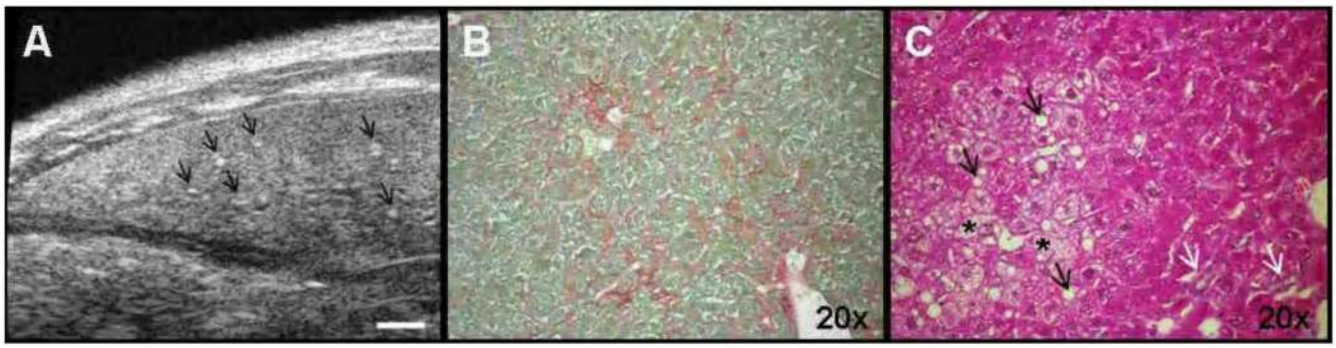

Figure 4. Features of altered hepatic parenchymal architecture in mice

Representative ultrasound (US) images and histologic sections of altered hepatic parenchymal architecture in a GNMT-KO mouse (8 months). Bar on US image 1 mm. Histologic sections magnification is 20×. A, US image of the left lobe of the liver showing heterogeneous hepatic echostructure, with alternating areas of low and high echogenecity and bright dots that correspond to fibrotic areas (arrows). B, Sirius red collagen staining with fibrotic areas in the liver (red areas). C, H/E histologic section showing enlarged hepatocytes with vacuolated cytoplasma (*), large nucleus and lipid acumulation (black arrows). Note the presence of small duct proliferation (white arrows).

Table 1

Ultrasonographic findings in the liver of MAT1A-KO and GNMT-KO mice over the time of the study

Ultrasonographic finding	Associated lesion	Number of cases in Experimental Groups[1] (incidence as %)				
		3 months (n=20)	5 months (n=17)	6 months (n=13)	8 months (n= 12)	15 months (n=9)
Homogeneous/isoechoic parenchyma	Normal hepatic parenchyma	**1** (5%)	**0** (0%)	**0** (0%)	**0** (0%)	**0** (0%)
Heterogeneous parenchyma	Fibrosis or altered parenchymal architecture	**2** (10%)	**8** (47%)	**10** (77%)	**12** (100%)	**9** (100%)
Increased parenchymal echogenicity	Diffuse steatosis	**8** (40%)	**6** (35%)	**3** (23%)	**3** (25%)	**2** (22%)
Hyperechoic nodules	Focal/Multifocal steatosis	**9** (45%)	**9** (53%)	**7** (54%)	**5** (42%)	**3** (33%)
Anechoic nodules	Biliary cysts	**0** (0%)	**0** (0%)	**0** (0%)	**0** (0%)	**4** (44%)
Hypoechoic nodules	Early stage HCC	**0** (0%)	**0** (0%)	**1** (8%)	**5** (42%)	**3** (33%)
Heterogeneous echogenicity nodules	Cellular alteration foci, Adenoma or advanced HCC	**0** (0%)	**0** (0%)	**4** (31%)	**6** (50%)	**9** (100%)
Bulging isoechoic nodules	HCC	**0** (0%)	**0** (0%)	**0** (0%)	**1** (8%)	**2** (22%)

HCC: hepatocellular carcinoma.

[1] Control animals (n=20) showed homogeneous and isoechoic hepatic parenchyma along the study (data not shown).

Ultrasound Med Biol. Author manuscript; available in PMC 2012 July 1.